

An Edge Sensor Design for the Thirty Meter Telescope

Terry Mast^a, Gary Chanan^b, Jerry Nelson^a, Robert Minor^c, Richard Jared^c
a University of California, Santa Cruz CA 95064 , b University of California, Irvine CA 92697
c Lawrence Berkeley National Laboratory, Berkeley CA 94720

ABSTRACT

The Thirty Meter Telescope project will design and build a thirty-meter diameter telescope for research in astronomy at optical and infrared wavelengths. The highly segmented primary mirror will use edge sensors to align and stabilize the relative piston, tip, and tilt degrees of freedom of the segments. We describe an edge sensor conceptual design and relate the sensor errors to the performance of the telescope as whole. We discuss the sensor calibration, installation, maintenance, and reliability.

Keywords: telescope, mirror, segment, sensor

1. INTRODUCTION

The primary mirror of the Thirty Meter Telescope (TMT) is an array of 738 nearly identical hexagonal mirror segments. The surface of the primary is a ellipsoid of revolution, and the surface of each mirror segment is an off-axis portion of that surface¹. The size and prism shape of the segments vary by about 1%, depending on their position in the array².

The lateral degrees of freedom (two translations of the segment center in the surface of the hyperboloid and rotation about the normal to the surface at the segment center) are constrained passively by the steel primary mirror cell. The remaining three degrees of freedom (motion along the segment normal and rotations about the two axes perpendicular to the normal) are actively controlled.

The control consists of two functions: alignment and stabilization. The alignment function is carried out by the alignment and phasing system (APS) using star light to determine desired values of the three degrees of freedom of the segments with respect to each other to an accuracy of a few nanometers. The stabilization maintains those degrees of freedom in the face of gravity and temperature changes and to some extent wind forces.

The stabilization is carried out using three actuators behind each segment and six edge sensors at the segment edge that measure the relative position of the segment with respect to its adjacent neighbors. In this report we describe a conceptual design for the edge sensors. This report is a summary of a more detailed report³ that includes the derivation of equations and motivations for the design.

The sensor requirements are described by Jared and Minor⁴, and this design attempts to address those requirements. The TMT error budgets⁵ call for an rms sensor noise of about 5 nm.

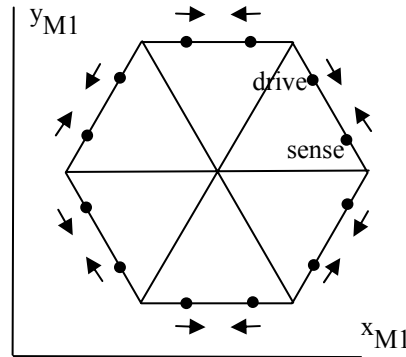
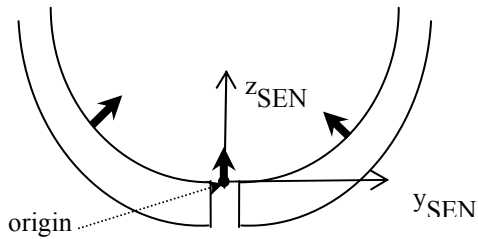
2. POSITION ON THE SEGMENT

An edge sensor consists of a sense half at the edge of one segment and a drive half at the edge on the adjacent segment. There is a sense half and a drive half for each side of the hexagon, alternating drive and sense.

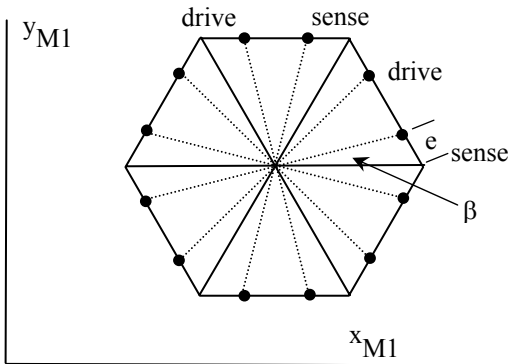
We assume the segment is a regular hexagon. The origin of the sensor coordinate system⁶ is at the z height of the reflecting surface and at the x,y positions shown below. Each sensor has its own coordinate system. At each origin the normal to the reflecting surface defines the z-axis of the sensor coordinate system.

Exaggerated side view of two adjacent segments. Bold arrows are normals to the reflecting surface.

The x axis is parallel to the hexagon side, and directions of positive x are shown below.



The hexagon sides shown above are at the mid-planes of the inter-segment gaps.

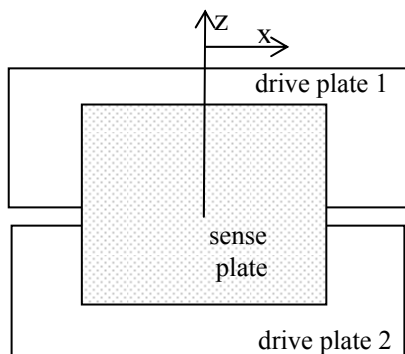


The distance e is identical for all sensors and all segments. The angle β is given by $\tan \beta = \sqrt{3}e / (2a_j - e)$; where a_j is the center-to-vertex distance of segment j .

3. OVERALL DESCRIPTION

Each sensor uses a change in the charge on a capacitor to measure a linear combination of

- 1) a change in the relative height (δz) of the two adjacent segments and
- 2) a change in the dihedral angle ($\delta \omega$) between the two adjacent segments.



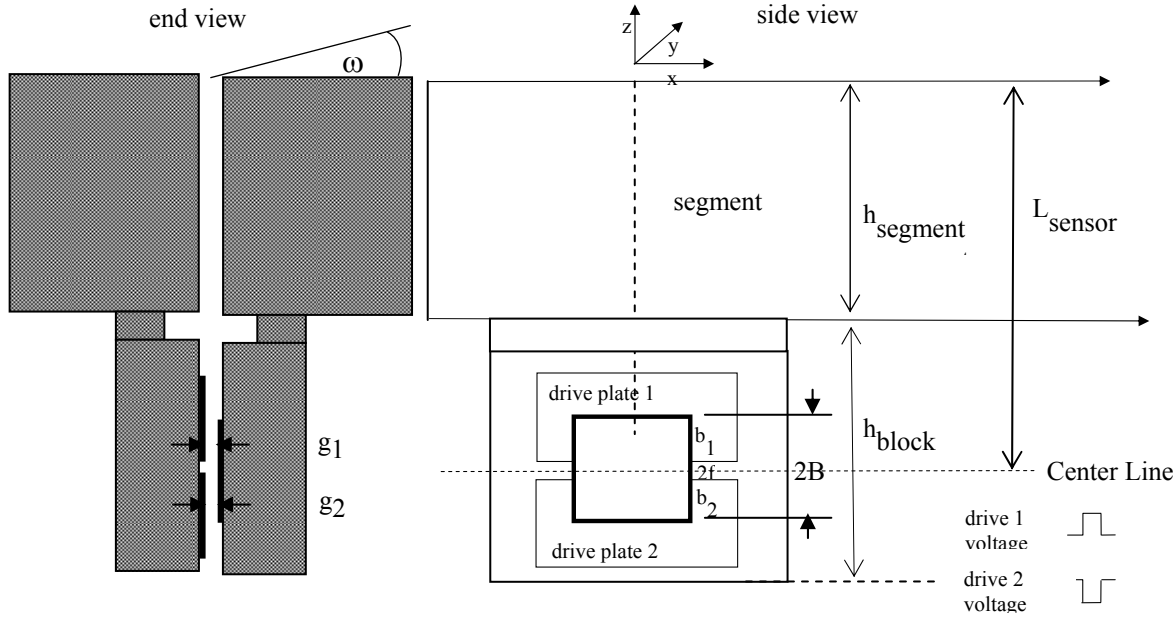
Capacitor plates (not to scale).

The sense plate is on one segment and the drive plates are on the other. Each half (drive or sense) is a single block of low thermal expansion glass-ceramic plated with capacitor plates. Each block is attached to the back of a segment.

4. SENSITIVITIES

We describe the sensor sensitivity to all six degrees of freedom of one segment with respect to the adjacent segment; translations δx , δy , δz and rotations $\delta\theta_x$, $\delta\theta_y$, $\delta\theta_z$. For a simple capacitor $C = Q/V = \epsilon A/g$, where C = capacitance, Q = charge, V = voltage, $\epsilon = 8.85e^{-12}$ (farads/m), A = plate area, g = gap between plates.

The proposed sensor geometry is shown below (not to scale).



The basic concept is similar to the capacitive sensor used for the Keck telescopes; a vertical motion of one segment will increase one capacitance while decreasing the other. This will be highly linear in the displacement and dihedral angle changes for the small changes that will occur. We calculate the detailed geometry of the proposed TMT sensor design using the two simplifying assumptions.

1. The capacitance is that of a simple capacitor in air. This is not strictly true since the glass-ceramic substrate has a dielectric constant. This reduces the capacitance by a factor up to about 2; calculated using the simulation code Maxwell. Consequently, to avoid this reduction we propose here to add ground planes to all sides of the sensor block with a 1 to 2 mm gap between the ground planes and active capacitor plates. Simulation of this configuration gives capacitances and sensitivities that agree within 1% of those calculated using the simple formulas used above.

2. The dielectric constant of the glass-ceramic substrate will enhance the coupled capacitance between the two drive plates. For the separation of the plates assumed below (4 mm) the coupled capacitance is small.

Sensitivity to relative segment motions δz and $\delta\theta_x (= \delta\omega)$

Although the design calls for symmetry in the plate dimensions, fabrication errors will result in small differences leading to non-zero values for $\Delta\Delta B$, $\Delta\Delta\omega$, $\Delta\Delta\omega$ and $\Delta\Delta G$ defined as follows.

Distances B and ΔB : $b_1 = B - f + (\Delta B + \delta z)$ and $b_2 = B - f - (\Delta B + \delta z)$

Dihedral angle between segments: $\omega = \Delta\omega + \delta\omega$

Distances G and ΔG : $g_1 = G + \Delta G + (L_{\text{sensor}} - f - b_1/2)(\Delta\omega + \delta\omega)$

$g_2 = G + \Delta G + (L_{\text{sensor}} + f + b_2/2)(\Delta\omega + \delta\omega)$

Drive voltages V and ΔV : $V_1 - V_2 = 2V$ and $V_1 + V_2 = 2\Delta V$

The sensor reading $R = Q_1 + Q_2 = [2\epsilon\epsilon_0 B V / G] [\Delta V / V + (\Delta B + \delta z) / B + (B + f)(\Delta\omega + \delta\omega) / 2G]$

The alignment/phasing processes tune $\Delta V (= V_{\text{offset}})$ to achieve $\Delta V/V + \Delta B/B + (B+f) \Delta\omega/2G = 0$

Afterwards the segment stabilization system uses the reading change δR to move the segments to correct small non-zero values δz and $\delta\omega$.

$$\delta R = [2\varepsilon \square V/G] [\delta z + (B(B+f)/(2G)) \delta\omega]$$

Define $L_{\text{effective}} = B(B+f)/(2G) \Rightarrow \delta R = [2\varepsilon \square V/G] (\delta z + L_{\text{effective}} \delta\omega)$

Sensitivity to $\delta\theta_z$

A rotation about the z axis to first order will not change the average gap and will have no effect on the final charge developed on the sense plate. The next order effect is negligibly small ($\delta C/C \sim 0.2 \times 10^{-10}$).

Sensitivity to $\delta\theta_y$

Consider the segment rotated about y, such that the other sensor on the same segment edge reads a maximum of it's operating range. A calculation for our proposed sensor shows the false reading generated by this rotation is $\sim 10^{-14}$ m, negligibly small.

Sensitivity to δx

The drive plates are intentionally wider than the sense plate in order to make the output insensitive to small δx . Second order fringe-field effects are expected to cancel and only negligibly small third order fringe-field effects will contribute. A potentially significant δx sensitivity is created if a fabrication/installation error introduces a difference in θ_y between the sense plate and the drive plates, θ_{y-d-s} . Then a gravity-induced or temperature-induced change in x (δx) causes a reading change corresponding to $\delta z_{\text{false}} = \delta x \theta_{y-d-s}$. Assume the sense plate has width = 30 m and is applied to an accuracy of 10 microns rms at the corners with respect to the block then $\theta_{y-d-s} = 0.010/15 = 7 \times 10^{-4}$ radians rms. If $\delta x = 0.1$ mm. $\Rightarrow \delta z_{\text{false}} = 70$ nm rms. This is a large effect, and will be removed using a fit to all gap measurements to establish the value of δx to < 5 microns and a fit to temperature and zenith angle to refine this to δx to < 1 micron, resulting in $\delta z_{\text{false}} < 0.7$ nm rms.

Sensitivity to $\square \delta y (= \text{gap change} = \delta G)$

Since the gap (G) will vary with gravity and temperature (resulting in changing the sensor output), we also need to measure G. We address below 1) the sensitivity to gap changes, 2) the expected size of the changes, 3) a method to measure the gap, and 4) the processing of the measurements. The gap measurement will be used to digitally correct the reading δR .

1) Sensitivity to gap changes. There are three ways a change in the gap (δG) affects the reading δR .

- It changes the sensitivity to δz . $\delta R/\delta z = 2\varepsilon a V/G$ $\delta(\delta R/\delta z) = (\delta R/\delta z)(-\delta G/G)$
- It changes the sensitivity to $\delta\omega$ $\delta R/\delta\omega = 2\varepsilon a V B(B+f)/(2G^2)$ $\delta(\delta R/\delta\omega) = (\delta R/\delta\omega)(-2\delta G/G)$
- It means the offset voltage is erroneous

$$V_{\text{offset}} = -V[\Delta B/B + (B+f)\Delta\omega/(2G)] \quad \delta V_{\text{offset}} = -V(B+f)\Delta\omega \delta G/(2G^2)$$

$$\delta R = 2\varepsilon B \delta V_{\text{offset}}/G = -2\varepsilon V B(B+f)\Delta\omega \delta G/(2G^3)$$

where $\Delta\omega$ is the dihedral angle between segments after segment installation.

In terms of a comparable δz $\delta z = -B(B+f)\Delta\omega \delta G/(2G^2)$

2) Expected size of gap changes.

- Temperature-induced: If the cell temperature changes by 10°C , then $\delta G = 125$ microns.
If we assume a rate of 1°C per hour, then $\delta G/dt = 3.5$ nm/second.

Gravity-induced: If the primary mirror moves by ~10 mm, and we assume that 10% is differential, then $\delta G \sim 1\text{mm}/30\text{m} = \sim 30$ microns.
 If this happens during a zenith to horizon slew in 2 minutes, then $\delta G/\text{dt} = 250$ nm/second.

We assume: • a maximum gap change of 150 microns $\Rightarrow \delta G/G = 0.15/2.0 = 0.075$
 • a maximum rate of 250 nm/second.

Using these values

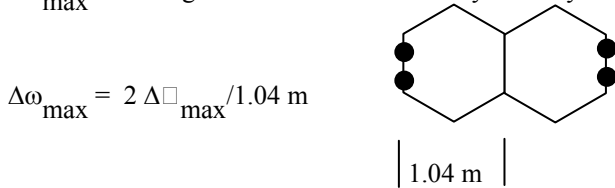
- Change in sensitivity to δz . $\delta G/G = 0.075$
- Change in sensitivity to $\delta \omega$. $2\delta G/G = 0.15$

These changes in sensitivity (1.075 and 1.15) change the convergence rate of the segment stabilization control. However, they are minor compared to gain of the control system (typically 0.2 to 0.1).

- Erroneous offset voltage. In terms of a comparable δz , $\delta z = -B(B+f) \Delta \omega \delta G / (2G^2)$
 \Rightarrow We want $\delta G/G < \delta z_{\text{max}}^2 G / [B(B+f)\Delta \omega_{\text{max}}]$

We want stability to $\delta z < 3$ nm. The $\delta G/G$ limit then depends on the installation error $\Delta \omega_{\text{max}}$.

For a maximum installation error Δz_{max} , the following diagram shows an **extremely** conservative estimate of $\Delta \omega_{\text{max}}$. The diagram assumes the extremely unlikely configuration with all four sensors at the maximum Δz_{max} .

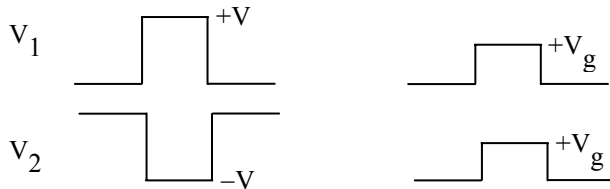


If $\Delta \square_{\text{max}} = 30$ microns, then $\Delta \omega_{\text{max}} = 6 \times 10^{-5}$ radians. If $B = 15$ mm, $f = 2$ mm, $G = 2$ mm, then $\delta G/G < 1/1275$.

We require the gap to be measured to this level from one alignment/phasing procedure to the next; ~several weeks.

3) Measuring the gap.

The sensor electronics are described below. We will measure the gap by modifying at 20Hz the drive voltages for 1 pulse of the 10 kHz square wave; equal to 2 of the 1000 charge pulses (both edges of the square wave give a charge pulse), and then average the 2 pulses.



The modification will reverse the sign of V_2 and reduce the voltage to $V_g = 1.0$ V to prevent saturation.

The reading during the gap measurement using a single pulse will be $R = Q_1 + Q_2 = \epsilon V_g 2(B-f)w/G$.

Assume $B = 0.015$ m, $f = 0.002$ m, $w = 0.030$ m, $G = 0.002$ m, $\epsilon = 8.85 \times 10^{-12}$, $V_g = 1$ volts. Then

$R = 3.5 \times 10^{-12}$ Coulombs = 2.2×10^7 electrons, and averaging 2 charge pulses gives 4.4×10^7 electrons. The error from electron statistics alone is $\delta R/R = 1/N_e^{1/2} = 1/9300$. For the error from ADC bit size assume a signal of 2000 counts for the 2 mm gap, and assume the rms error for 1 LSB = $12^{-1/2} = 0.29 \Rightarrow \delta G/G = 1/6900$.

Both of these are smaller than our goal of 1/1275, thus averaging only two charge pulses is sufficient.

4) Processing the Measurements

We will use the local temperature (T), the elevation encoder reading (el), and the sensor gap measurement (G), to create a local sensor-by-sensor correction to the raw sensor reading.

[We will also use the APS measurements, the gap measurements, the elevation encoder reading (el), and the temperature measurements (T) to create a **Global look-up table** of desired sensor readings as a function of T and el.]

With 4212 gap measurements and $(3 \times 738 - 3)$ in-plane segment degrees of freedom, we are highly over constrained. We will make a fit to the ensemble of gap measurements to determine their consistency and the measurement error. We will use the fit to all gap measurements to establish the best estimate of the gap for each sensor and an estimate of the temperature of the mirror cell. Smooth functions of el and T will be fit to the measurements made at many values of el and T , and a correction for each sensor will be constructed from the fits. We expect the residuals to the lookup tables will be random and thus correspond to random sensor noise. We want the residuals to be less than ~ 3 nm rms.

Temperature

In addition to direct temperature measurements, we will also use the average gap measurement as a measure of the average cell temperature. The lowest order effect of temperature is a uniform change in the temperature of the mirror cell. The gap change is the same for all gaps (uniform expansion or contraction of the cell). Using the average of all gap measurements we will create a highly precise lookup table versus temperature. The error of each sensor gap (σ_G) can be made small by averaging over time. In addition, the error on the average over all sensors further reduces the measure of this single mode: $\sigma_G / 4212^{1/2} = \sigma_G / 65$. If the sensor readings were not corrected for this, then the readings would be erroneously interpreted as a focus-mode deformation of the primary mirror array.

5. CAPACITOR PLATE DIMENSIONS

Drive Plate Design

Width (w_{drive}) To make the reading insensitive to motions along the x-axis (δx),

we use a drive plate width that extends beyond the sense plate by 5 mm (see below).

Height (h_{drive}) To accommodate the sensor range in z and make the reading insensitive to rotations about the y-axis

($\delta \theta_y$), we use drive plate heights that are smaller than the sense plate by 3.0 mm (see below).

Drive Plate Separation ($2f$) To maintain a small capacitive coupling between the two drive plates, we use a plate separation of 4 mm corresponding to $f = 2$ mm.

Sense Plate Design

In the design calculations we have assumed the simple capacitance formulas and assume ground planes surround the capacitor plates. A simulation program "Maxwell" confirms the simple formulas are accurate.

Width (w_{sense})

We compare the δz sensitivity with the sensors being used on the Keck telescopes.

$$TMT/Keck = [w_{sense}^{tmt} V^{tmt} / G^{tmt}] / [A^{keck} V^{keck} / (G^{keck})^2]$$

$$A^{keck} = 30 \times 30 = 900 \text{ mm}^2 \quad V^{keck} = 6.74 \text{ volts} \quad G^{keck} = 4 \text{ mm} \quad G^{tmt} = 2 \text{ mm}$$

We propose here for the TMT $w_{sense}^{tmt} = 30$ mm, $V^{tmt} = 6$ volts.

$$TMT/Keck = \sim 1/4$$

Height (h_{sense})

control-stabilization :

The maximum δz range is $\sim 2(a/t) act_{max}$, where $a = 0.6$ m, $t = 0.31$ m, $act_{max} = 3.4$ mm is the maximum

actuator range maximum $\delta z \sim 15$ mm. However, Even if the sensors saturate the stabilization will converge.

control-stabilization :

This is dominated by the need to use focus-mode and three-color mode for alignment.

Focus mode is "edge continuous" so it shouldn't require δz motions. Three-color mode is used to

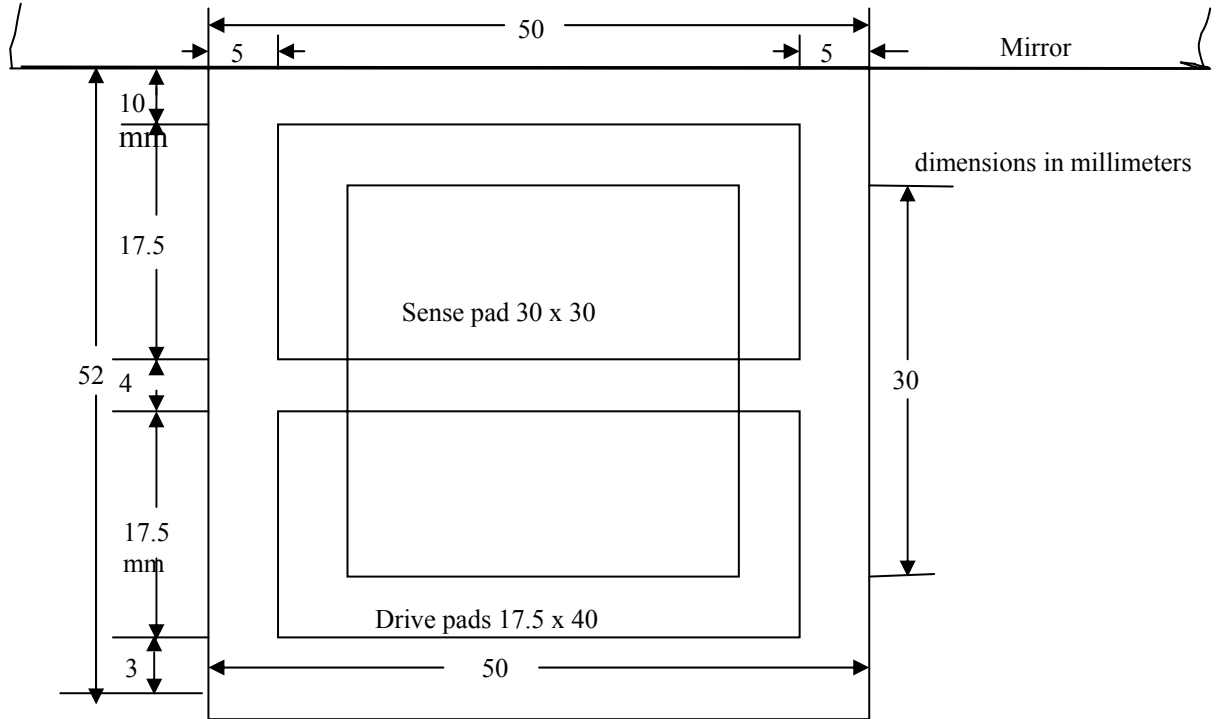
- capture pistons for installation misalignment errors in sensor alignment lookup table (< 10 microns)

Conclusion: The range must be perhaps a few times the offset range.

sensitivity to dihedral angle $\delta\omega$.

Assume $G = 2 \text{ mm}$, $B = 15 \text{ mm}$ ($h_{\text{sense}} = 2B$), $f = 2 \text{ mm}$ (plate separation = 4 mm)

$$L_{\text{effective}} = B(B+f)/(2G) \Rightarrow L_{\text{effective}} = 63.8 \text{ mm}$$



With these dimensions the capacitance from the overlap with one drive plate is 1.73 pF.

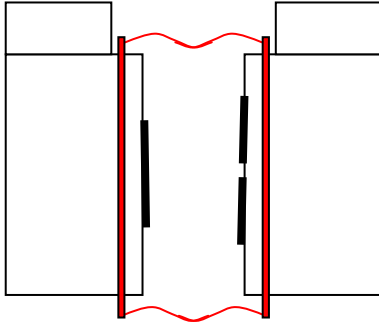
6. MECHANICAL DESIGN

The sensor substrate is a rectangular block of glass-ceramic or ULE with dimensions in the table below. All sides are polished to relieve stress. All edges are beveled.

Three raised feet on each block contact the shined spherical back of the segment. A rare earth magnet is bonded to the block. This attracts a similar magnet bonded to the back of the segment and holds the block in position on the segment. The block may be positioned using nylon pins protruding from two blind holes drilled into the back of the segment. One pin seats in a blind hole in the block and the other rests against the edge of the block. Alternately, registration blocks attached to the mirror back may be used, thus eliminating the need for holes in the mirror.

Three holes through the block thickness provide paths for wires to connect to the sense and power plates. Thus all electronics connect to the back of the sense block.

A method to keep the gap isolated from dust, water, and water vapor is critical to the performance. We leave a space between the plate side of the block and the segment of $5 \times 5 \times 50 \text{ mm}$ for a barrier we call the "gaiter". A flexible torus of material can be inserted through the gap and connected around each block in this space. The figure below illustrates the concept.



A collapsed gaiter might be stored on one block of one side of the sensor for segment installation, and then for segment use it might be deployed across the gap either manually or using air pressure or an electromagnet. An explicit design is remains to be created.

The mechanical dimensions follow.

Each Block

dimensions	(mm)
length (along edge of segment)	50
depth (extending behind segment)	45
(boot space 5, capacitor space 40)	
thickness	20
(15 mm at boot space)	
edge bevels (12)	0.3
feet (3)	
length	4
widths (2)	2
width (1)	4
height	1
hole for rare earth magnets	
diameter	10
depth	7
hole for positioning pin	
diameter	3
block volume (m ³)	4.5E-05
block mass (kg)	0.114

Sense Block

	(mm)
feed through hole (1)	
diameter	2
sense plate	
Z height	30
X length	30

Drive Block

	(mm)
feed through holes (2)	
diameter	2
drive plates (2)	
Z height	17.5
X length	40

Comments.

Feet (3): The compression induced by the magnet force will not compress the feet to match the curved segment surface. The feet must be polished on a curved tool (radius ~ 60 m) to seat properly.

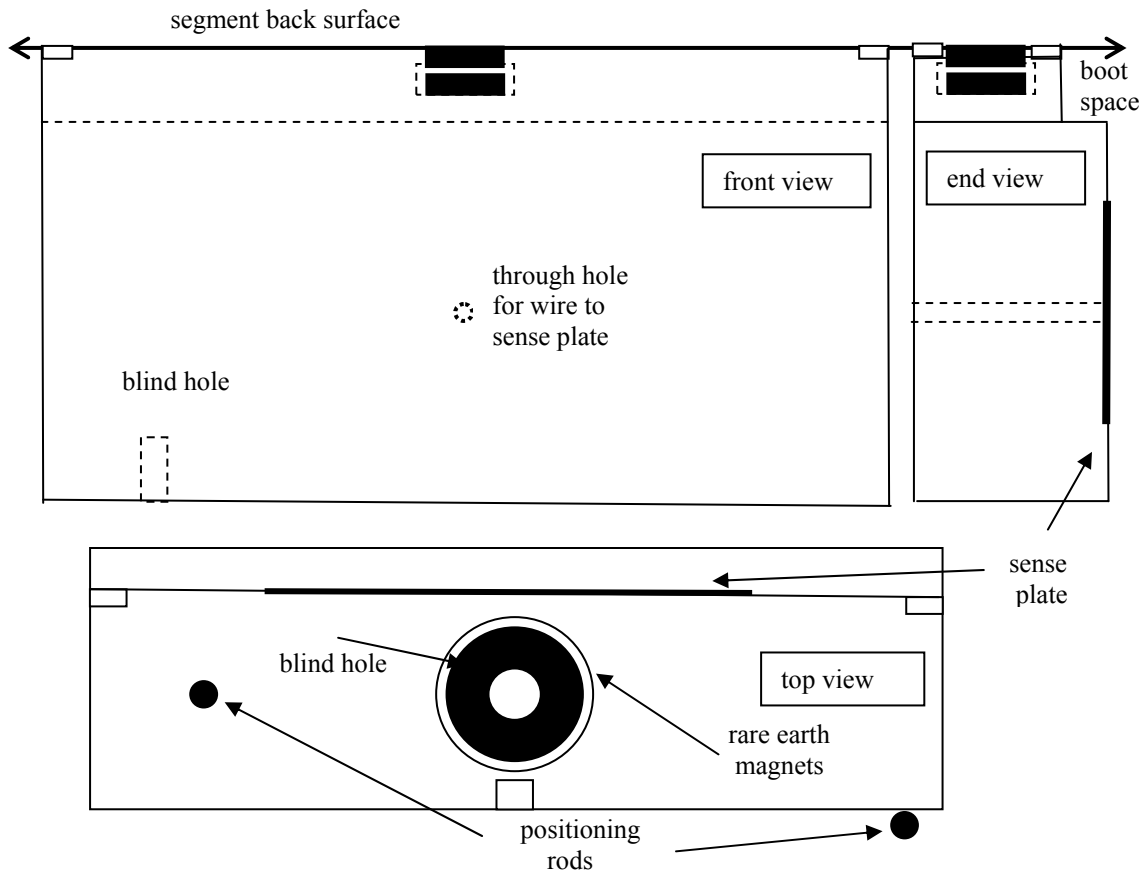
In addition, the feet heights must match the spherical surface slope and the normal at the gap for the block to be at an angle such that the gap is uniform. The spherical surface slope at the edge is $\sim a/k = 0.6/60$, and over the block thickness (20 mm) gives a difference in feet height of 200 microns. The nominal height is 1 mm, but the actual heights must provide this 200 micron difference.

Surfaces: all are fine ground

Capacitor plates: coating: 0.5 microns of gold over 0.05 microns of chrome

Magnets: rare earth magnets: minimum required force $\sim 15 \times$ sensor mass = 1.5 kg ~ 15 N

We assume two magnet pairs/block with each magnet for a total of $(2)(12)(738)(7/6) = 20,700$ magnets.



7. ELECTRONICS (DESIGN, RANGE, LINEARITY)

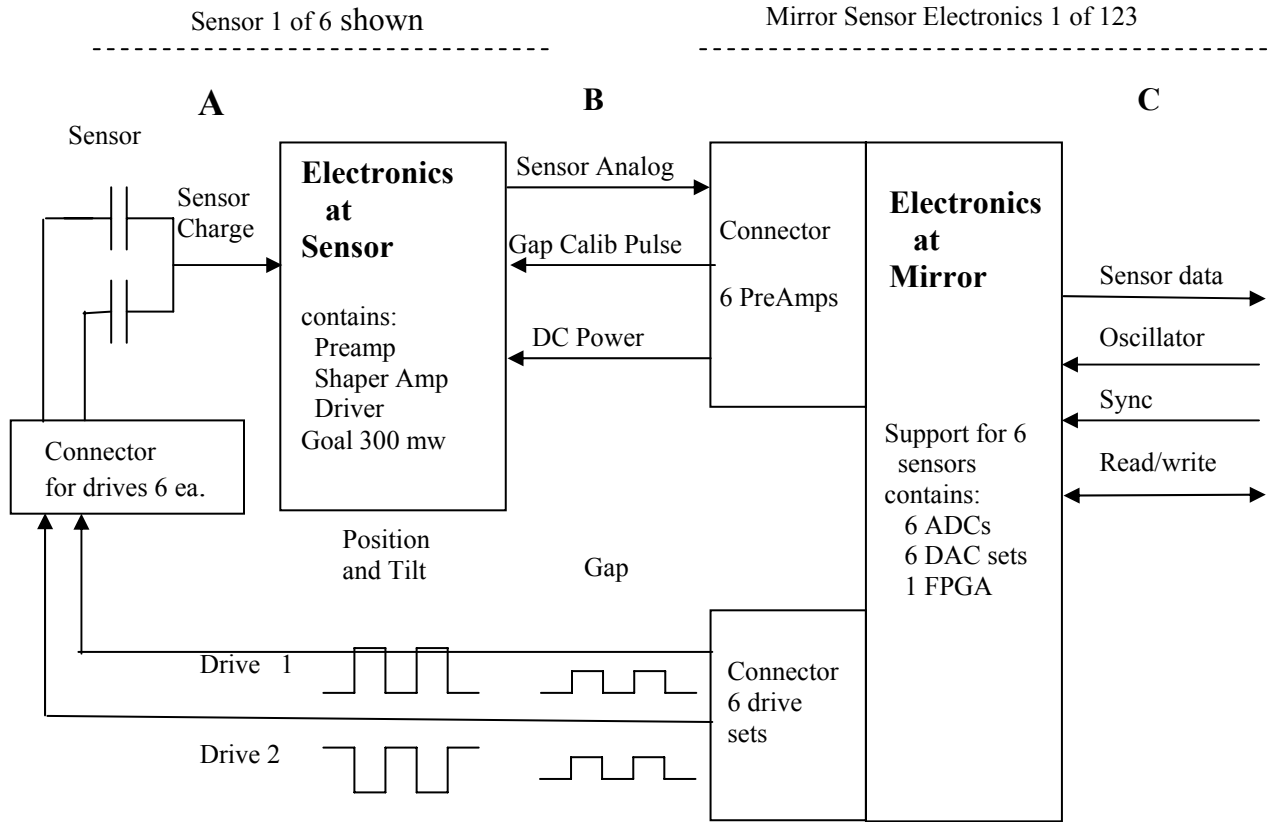
Design

The next three drawings show an initial design of the proposed sensor electronics.

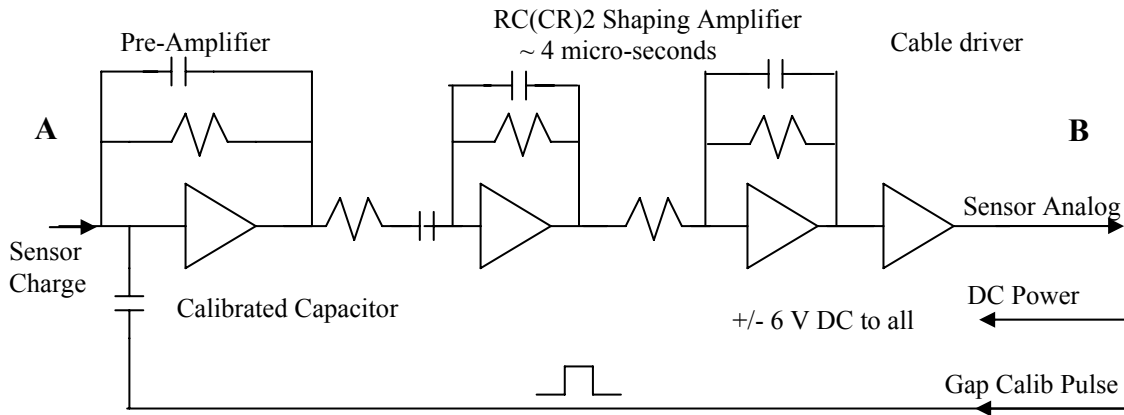
The sensor is connected to the Pre-Amplifier by a coax cable (0.3 to 0.6 m long). The electronics at the sensor fit on a 50 x 50 mm board that is permanently attached to the segment.

- Readout at 20 Hz has 1000 ADC data samples:
 - 998 samples are summed to measure position/tilt and 2 samples are used to measure the gap.
 - Both numbers are read at 20 Hz.
- The gap calibration pulse is used to obtain the ADC value for a gap of 2 mm.
- In "Fast Data Capture" mode the sensor is read at 400Hz, is locally stored and readout at a later time.

Electronics Overview

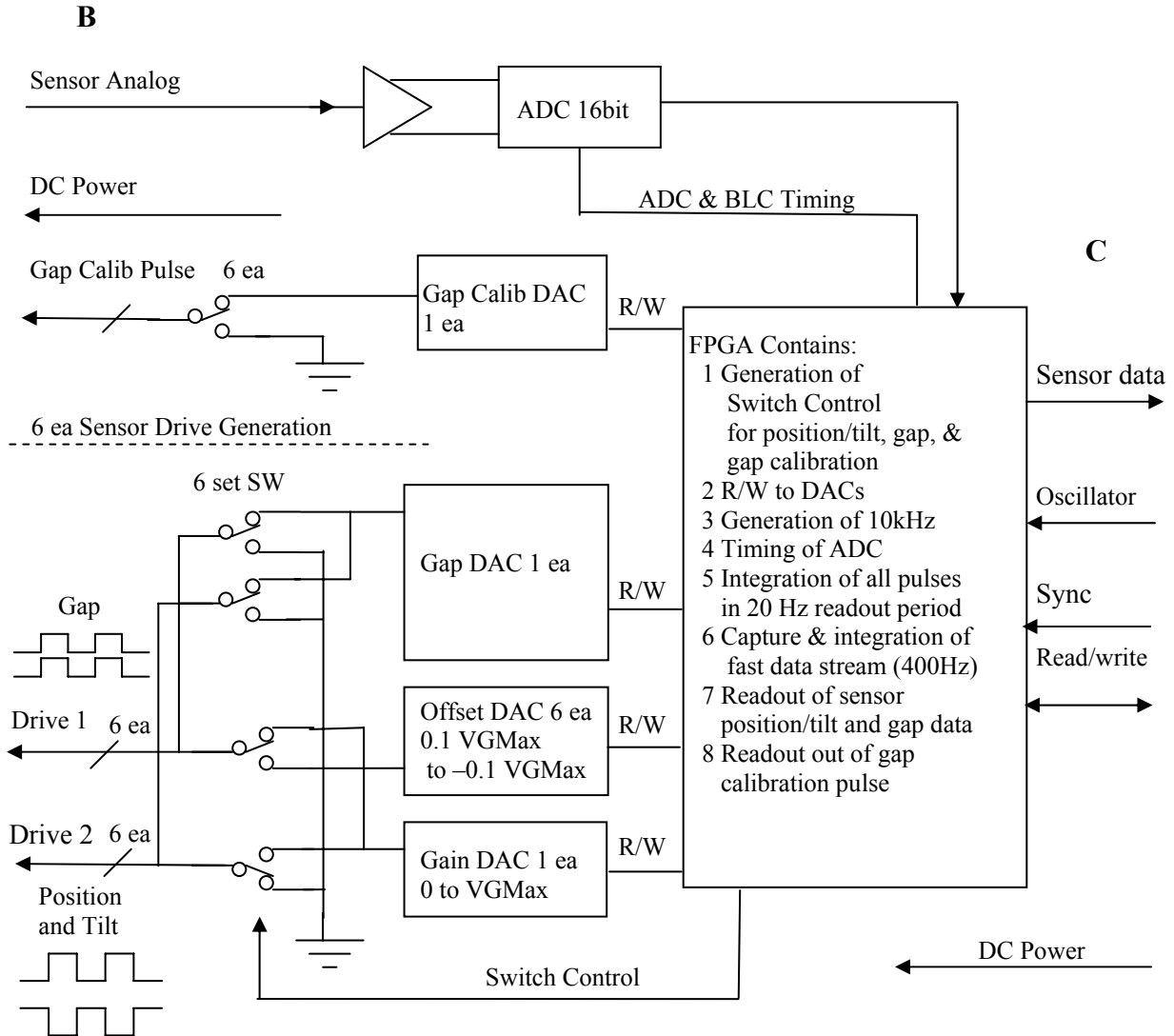


Electronics at Sensor



Electronics at Mirror

6 ea Sensor Support, BLC and ADC



Range

Using standard fixtures we will measure the position of the plates with respect to the reflecting surface after each sensor is attached to the segment. The initial offset voltages will be determined using these measurements. We assume the rms measurement error is 10 microns. To accommodate measurement errors and allow the phasing measurement to “capture” all segments, we assume the electronics requires a full range (in possibly a “coarse” mode) of ± 30 microns.

Linearity

We assume the non-linearity to be dominated by the non-linearity in the final ADC. Non-linearity caused by fringe fields and substrate dielectric constant is negligible. Commercial ADC's with 16 bits advertise a non-linearity of $<1\%$ of full range. Depending on the application of the sensor this may or may not need to be removed in software. For the sensor range during normal segment stabilization, non-linearity is negligible.

8. SENSOR NOISE

We assume a square wave pulse rate of 10kHz. We assume the averaging rate for segment stabilization will be 20 Hz (giving $(10\text{kHz} \cdot 2)/20 \text{ Hz} = 1000$ charge pulses per average) and for diagnostics (called “fast data capture “ mode at Keck) will be 400 Hz (giving 50 pulses per average).

For segment stabilization, the telescope error budget calls for a sensor electronic noise corresponding to $\sim 3 \text{ nm rms}$ δz . For $\delta z = 3 \text{ nm}$, $\delta C = 0.273 \text{ pf/mm}$ from Maxwell simulations and $V = 6 \text{ V}$, the charge from a single 3 nm pulse is

$$\delta Q = \delta C V = 31 \text{ electrons.}$$

The noise will be dominated by noise in the pre-amp, and we have determined using both simulation and calculation a noise of 90 electrons rms for each charge pulse. Since alternate pulses have opposite signs, the base line is removed, and the signals from 1000 pulses are added. The signal-to-noise ratio is $S/N = (3 \text{ electrons} \cdot 1000)/(90 \text{ electrons} \cdot 1000^{1/2}) = 11$ corresponding to 0.3 nm rms . The Keck sensor electronics noise is $< 1 \text{ nm rms}$ ⁷.

9. SENSOR NOISE PROPAGATION TO PRIMARY MIRROR

A detailed description of the effect of sensor noise on the shape of the full primary mirror is given in Reference 3. A fundamental result is

$$80\%EE = \sigma_s [0.0065] \quad \text{with } 80\%EE \text{ in arc seconds on the sky and } \sigma_s \text{ in nm}$$

The TMT error budget calls for $80\%EE < 0.030$ arc seconds, requiring $\sigma_s < 4.6 \text{ nm}$. This gives rms surface $S_{\text{rms}} = 58 \text{ nm}$ and rms wavefront $W_{\text{rms}} = 116 \text{ nm}$. The implication of this value for the sensor requirements depends on the TMT control bandwidth. If we assume a bandwidth (BW) = 0.3 Hz and a white noise spectrum, then the required sensor noise (S_{noise}) is given by⁸

$$S_{\text{noise}} = \sigma_s / [(\pi/2) \text{ BW}]^{1/2} \text{ yielding} \quad S_{\text{noise}} < 6.7 \text{ nm}/\sqrt{\text{Hz}}^{1/2}$$

10. POSITION SENSITIVITY

We assume the magnets will hold the sensor in position during operations. The following are the tolerances for installation of the block on the back of the segment.

Δx	$< \pm 0.5 \text{ mm}$	To not add fringe field effects to capacitances
Δy	$< \pm 0.1 \text{ mm}$	To not significantly change the gap
Δz	$< \pm 0.03 \text{ mm}$	
$\Delta\theta_x$	$< \pm 3.0\text{e-}3 \text{ rad}$	(0.2mm/66mm) To not require too large an offset ΔG
$\Delta\theta_y$	$< \pm 2.5\text{e-}3 \text{ rad}$	(0.5mm/200 mm) To not add fringe field effects
$\Delta\theta_z$	$< \pm 5.0\text{e-}4 \text{ rad}$	(0.1mm/200 mm) To not add fringe field effects

11. GRAVITY SENSITIVITY

Gravity changes from zenith to horizon will change the sensor reading, resulting in relative motions of the sense and drive blocks, in two ways:

- deformation of the segments
- bending and tilt of the sensor

A priori we expect the first to dominate, since the drive and sensor block will move under lateral gravity in opposite directions. We expect the bending and tilt of the sensors to be in the same direction canceling the effect on the sensor reading.

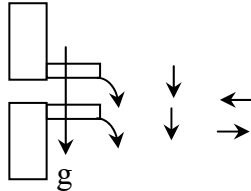
Deformation of the Segments: Axial gravity

The axial component of gravity acting on the sensor blocks will deform the segment. To first order, this will be corrected by re-optimizing the positions of the whiffletree/segment attachment points. Any residuals will be corrected at

the zenith using ion figuring. This will result in a surface deformation as the zenith angle increases. However the overall error budget increases with zenith angle, and this particular term can increase substantially. We anticipate that this axial gravity term will readily meet the error budget.

Deformation of the Segments: Lateral gravity

Because the sensors extend in back of the segment, lateral gravity will induce a moment on the edges of the segments. Relative motions of the sensor blocks will be in the same direction in the plane of the segments, but in opposite directions normal to the segments.



We will make a finite element calculation to estimate the magnitude of this effect. However, it will be removed using the APS-generated lookup table (a function of zenith angle). In addition, the error budget allows the error to increase substantially with increasing zenith angle. The residual error from the lookup table will make a negligible contribution to the error budget.

Bending and tilt of the sensor

Under gravity loads in the x and y directions the body will bend and the feet will compress. Since the drive and sense halves are identical, the effects will cancel and have a negligible effect on the reading. In addition, if there is any residual effect, it will be smoothed with a fit to a function of elevation angle and be removed in the APS-generated lookup table.

We have calculated the magnitude of the bending and tilting effects that will be cancelled. The sensor bending under its own weight is for gravity in the x and y direction is 0.3 and 2.2 nm respectively.

At elevation angle = 0 the sensor will tilt since the force on one foot will increase (δF) and on the other decrease ($-\delta F$). Balancing the moment gives a maximum displacement of 10.2 nm. The force applied to each foot by the magnet is about 15 times the sensor weight; $F_{\text{axial}} = 0.114 (9.8) 15 / 2 = 8.4 \text{ N}$

At the horizon, the force on the upper foot is reduced by 1.8 N (~20%) and the force on the lower foot is increased by 1.8 N. The friction between the feet and the segment must be adequate to prevent creep motion of the sensor as the telescope is repeatedly moved over a large range in zenith angle.

12. TEMPERATURE SENSITIVITY

The mechanical sensor is made of low thermal expansion glass ceramic with a CTE that will closely match the CTE of the segment. Small differences in CTE might lead to a sensitivity up to $\sim 10 \text{ nm}/^\circ\text{C}$, and this will be removed by calibration. The residual will not contribute significantly to the temperature sensitivity. The temperature sensitivity of the readout electronics depends on the selection of components. As a guide, the rms temperature sensitivity of the Keck sensors⁷ is about $0.3 \text{ nm}/^\circ\text{C}$.

13. HUMIDITY SENSITIVITY

We do not yet have a definitive understanding of capacitive sensor sensitivity to humidity.

- Observers at Keck have never suggested that the humidity degrades the performance.
- Recent laboratory tests of a Keck sensor show a sensitivity to humidity that depends on the nature of the process used to clean the gold surfaces. Gold has a high free surface energy, and it condenses water with a low free energy surface. Gabor Somoraji (UC Berkeley) has suggested the possibility of coating the gold with a hydrocarbon or Teflon, and we will investigate this possibility.

14. POWER

Our goal is to have the power radiated by each sensor and its electronics to be < 300 mW. In addition, we require that the electronics/software allow a complete recovery from a power loss of the settings at the time of the loss. A full electronics design is being created to meet these requirements.

15. DRIFT WITH TIME

The sensors are required to not drift during the periods between segment alignment/phasing procedures, roughly every six weeks.

In addition, since we will want to use the array as soon after segment exchange as possible, we have set a goal for the full sensor system to settle to its final value in less than four hours. We expect that during segment exchange the mechanical part of the sensor will have been undisturbed from many hours and will have a very small settling time. The electronics should be largely insensitive to temperature, and we also expect a small settling time.

16. MAINTENANCE

There are three categories of activity that will affect the sensor reading and require a calibration using the APS.

1. Sensor removal and replacement
2. Segment surface cleaning
3. Segment removal, coating, and replacement

1. Sensor removal and replacement

The exchange of a sense block, drive block, or the electronics for a sensor will require one or more measurements by the APS to re-establish the desired sensor reading.

2. Segment surface cleaning

The cleaning of a segment surface with CO_2 or other agents can potentially affect a sensor reading. This will require APS measurements to confirm the segment cleaning process does not affect the desired sensor reading. If the cleaning process has been repeatedly shown to not affect the reading, the use of the APS after cleaning can be discontinued.

3. Segment removal, coating, and replacement

The effect of the sensor on the coating chamber and the effect of the coating process on the sensor need to be thoroughly proven and understood. Potential concerns include the heat generated by the segment coating process, out-gassing of either the sensor or the segment and its support, and changes in the sensor's gold coating.

Removal and replacement of a segment will change the gap (ΔG). This alone will require measurements by the APS to re-define the desired sensor reading.

Removal and replacement of a segment will change the values of Δz and $\Delta \omega$. A database of matching drive block and sense block serial numbers may be used to improve the efficiency of APS measurements.

17. RELIABILITY

The piston, tip, and tilt degrees of freedom of the 738 segments are actively controlled by 2214 actuators and 4212 sensors. Thus there is extensive redundancy in the sensor measurements. At any one time many sensors could be deleted from the system, and the stabilization performance would not significantly degrade. The Keck telescopes typically operate with several sensors deleted from the control algorithm.

ACKNOWLEDGEMENTS

The authors gratefully acknowledge the support of the TMT partner institutions. They are the Association of Canadian Universities for Research in Astronomy (ACURA), the Association of Universities for Research in Astronomy (AURA), the California Institute of Technology and the University of California. This work was supported, as well, by the Canada Foundation for Innovation, the Gordon and Betty Moore Foundation, the National Optical Astronomy Observatory, which is operated by AURA under cooperative agreement with the National Science Foundation, the Ontario Ministry of Research and Innovation, and the National Research Council of Canada.

REFERENCES

The central archive of TMT documents (Docushare) is at tmt.org. TMT Reports and Technical notes are available at tmt.ucolick.org

1. Mast, T., J. Nelson, and G. Sommargren, "Primary Mirror Segment Fabrication for CELT", TMT Report No. 5, Proceedings of the SPIE, 4003 (June 2000), document archive Docushare CEL.OPT.JOU.00.001.REL01
2. Mast, T. and J. Nelson. "TMT Primary Mirror Segment Shape" TMT Report No. 58 (November 2004) document archive Docushare TMT.OPT.TEC.04.001.REL01
3. Mast, T., Gary Chanan, Jerry Nelson, Robert Minor, Richard Jared "An Edge Sensor Design for the TMT" TMT Report No. 70 March 2006
4. Jared, Richard and Robert Minor, "TMT Position and Tilt Sensor Requirements" document archive Docushare TMT.SEN.SPE.05.001.REL02 (October 2005)
5. Mast, T. and J. Nelson , "Image Size and Wavefront Error Budgets" TMT Report No. 10, document archive Docushare TMT.OPT.TEC.05.024(,025, and 026).DRF01)
6. Mast, Terry , George Angeli, and Scott Roberts "TMT Coordinate Systems", TMT Report No 67, document archive Docushare TMT.SEN.TEC.05.016.DRF04 (2005)
7. Jackson, H.G. and T. T. Shimizu, (Position Sensor Electronics for the Ten Meter Telescope), Keck Observatory Technical Note No. 224 (April 1987) (LBL-23383)
8. MacMartin and Chanan, Control of the California Extremely Large Telescope Primary Mirror, TMT Report No. 40, 2002, TMT document archive Docushare CEL.CTR.TEC.02.001.REL01